Cuadernos de Investigación Geográfica *Geographical Research Letters*	2025	Nº 51 (2)	pp. 133-154	EISSN 1697-9540

http://doi.org/10.18172/cig.6889

POSTFIRE VEGETATION RECOVERY AND SPECTRAL SEPARABILITY OVER AMAZONIAN SAVANNA ECOSYSTEMS USING REMOTE SENSING TIME SERIES AND FUEL LOADS MEASUREMENTS

DANIEL BORINI ALVES[1]*, ANTONIO LAFFAYETE PIRES DA SILVEIRA[2], BRUNO CONTURSI CAMBRAIA[3], JOSÉ FALCÃO SOBRINHO[1], THIAGO SANNA FREIRE SILVA[4], FERNANDO PÉREZ-CABELLO[5]

[1] *Universidade Estadual Vale do Acaraú, Programa de Pós-Graduação em Geografia, Avenida John Sanford, 1845, 62030-000, Sobral, Ceará, Brazil.*

[2] *Universidade Federal de Rondônia, Programa de Pós Graduação em Conservação e Uso de Recursos Naturais, Departamento de Biologia, BR 364, Km 9.5, 76801-059, Porto Velho, Brazil.*

[3] *Instituto Chico Mendes de Conservação da Biodiversidade (ICMBio), Gerencia Regional 3 – Centro-Oeste, Rua 2 Quadra 30 Lote 36, nº 45/49, 74013-020, Goiânia, Goiás, Brazil.*

[4] *University of Stirling, Department of Biological and Environmental Sciences, FK9 4LA, Stirling, Scotland.*

[5] *University of Zaragoza, Department of Geography and Spatial Management, Geoforest-IUCA Group, C/ Pedro Cerbuna 12, 50009, Zaragoza, Spain.*

ABSTRACT. Monitoring and understanding vegetation responses to fire in Amazonian savanna ecosystems remains a very important scientific challenge to improve the landscape management practices of these areas. In this sense, the present study analyzes the dynamics of spectral separability as well as the postfire vegetation recovery process related to fire experiments carried out in open savanna ecosystems of the Campos Amazônicos National Park (Brazil). For this purpose, a harmonized Landsat and Sentinel-2 dataset was processed and analyzed. The time series of the Normalized Difference Vegetation Index (NDVI) and the Normalized Burned Ratio 2 (NBR2) spectral indices were also generated from this same dataset for the period from 2019 to 2023 and evaluated in combination with fine fuel load in-situ measurements. M-Statistics and mean absolute difference were calculated comparing data from burned and unburned plots, considering different treatments of fire seasonality (Early-Dry Season – EDS; Middle-Dry Season – MDS fires) and time since last fire (2-year-old fuel age; 3-year-old fuel age; and 10-year-old or older fuel age fires). The combined use of Sentinel-2 and Landsat resulted in an availability of cloud-free or partially cloud-free images ≈0.6 times greater than that obtained when using Landsat images exclusively. The potential of the NBR2 stood out, generating statistically significant mean absolute difference values when comparing EDS and MDS fires, and also when comparing 2-year-old fuel age areas with 3-year-old or 10-year-old or older fuel age areas. Satellite and field information converged in the detection of a rapid response of vegetation to fire in these ecosystems, demonstrating that conditions similar to those observed before the fire were reached after three rainy seasons. The results reinforce the potential of Landsat and Sentinel-2 harmonized remote sensing datasets to assess and monitor fire-affected areas over Amazonian savanna ecosystems, providing ecological meaning and establishing connections between remote sensing and field datasets.

Recuperación de la vegetación posincendio y separabilidad espectral en ecosistemas de sabana amazónica mediante series temporales de teledetección y mediciones de carga de combustibles

RESUMEN. El monitoreo y la comprensión de las respuestas de la vegetación al fuego en los ecosistemas de sabana amazónica siguen siendo un desafío científico muy importante para mejorar las prácticas de manejo del paisaje en estas áreas. En este sentido, el presente estudio analiza la dinámica de la separabilidad espectral, así como el proceso de recuperación posincendio de la vegetación, en relación con experimentos de fuego realizados en ecosistemas de sabana abierta del Parque Nacional Campos Amazônicos (Brasil). Para este propósito, se procesó y analizó un conjunto de datos armonizado de Landsat y Sentinel-2. También se generaron series temporales del Índice de Vegetación de Diferencia Normalizada (NDVI) y del Índice Normalizado de Quema 2 (NBR2) a partir de este mismo conjunto de datos para el período 2019–2023, evaluándose en combinación con mediciones in situ de carga de combustibles finos. Se calcularon M-Statistics y diferencia absoluta media comparando datos de parcelas quemadas y no quemadas, considerando diferentes tratamientos de estacionalidad del fuego (fuegos de inicio de estación seca – EDS; fuegos de mitad de estación seca – MDS) y tiempo desde el último incendio (combustible de 2 años; combustible de 3 años; y fuegos con combustible de 10 años o más). El uso combinado de Sentinel-2 y Landsat resultó en una disponibilidad de imágenes libres o parcialmente libres de nubes ≈0,6 veces mayor que la obtenida al usar únicamente imágenes de Landsat. El potencial del NBR2 se destacó, generando valores estadísticamente significativos de diferencia absoluta media al comparar incendios EDS y MDS, así como al comparar áreas con combustible de 2 años frente a las de 3 años o de 10 años o más. La información satelital y de campo coincidió en la detección de una rápida respuesta de la vegetación al fuego en estos ecosistemas, demostrando que las condiciones similares a las observadas antes del incendio se alcanzaron después de tres estaciones lluviosas. Los resultados refuerzan el potencial de los conjuntos de datos armonizados de teledetección Landsat y Sentinel-2 para evaluar y monitorear áreas afectadas por incendios en los ecosistemas de sabana amazónica, aportando significado ecológico y estableciendo conexiones entre los datos de teledetección y los de campo.

Keywords: Burned areas, Landsat, Sentinel-2, NBR2, NDVI, tropical savannas.

Palabras clave: áreas quemadas, Landsat, Sentinel-2, NBR2, NDVI, sabanas tropicales.

Received: 20 June 2025

Accepted: 19 August 2025

* **Corresponding author:** Daniel Borini Alves, Universidade Estadual Vale do Acaraú, Programa de Pós-Graduação em Geografia, Avenida John Sanford, 1845, 62030-000, Sobral, Ceará, Brazil. Email address: daniel_borini@uvanet.br

1. Introduction

The current climate change scenario has led to a significant increase in areas affected by fires globally (Burton *et al.*, 2024; Senande-Rivera *et al.*, 2022). This highlights the importance of carrying out studies focused on understanding the impact of fire and how the post-fire vegetation recovery process occurs in different types of landscapes (Archibald *et al.*, 2018). In Brazil, the Amazonian savannas are ecosystems under strong anthropogenic pressure, and knowledge of their vegetation characteristics is still very limited (Carvalho and Mustin, 2017).

Amazonian savannas are understood as a set of enclaves with a predominance of open natural vegetation physiognomies, with an ever-present herbaceous layer, which are biogeographically isolated by the extensive domain of Amazonian rainforests (Ab'Saber, 2003; IBGE, 2012; Prance, 1996). They cover a significant area of ≈15.3 million hectares in Brazilian territory (MAPBIOMAS, 2023), and their origin is mainly related to paleoclimatic inheritances existing in the areas of current disposition of the Amazon basin. The forested areas in this basin underwent successive moments of expansion and

contraction in relation to the areas of tropical savannas of Central Brazil (regionally called Cerrados) throughout the end of the Tertiary and mainly during the Quaternary (Ab'Saber, 1977; Carneiro Filho, 1993; Haffer and Prance, 2002).

The strong genetic connection between the flora of the Amazonian savannas and the Brazilian Cerrado (Prance, 1996; Ratter *et al.*, 2003), results in a flora that presents a series of mechanisms of resistance and resilience to fire (Simon *et al.*, 2009). The Cerrado is characterized as a biome with a history of evolution marked by the presence of natural fire regimes (Alves and Alvarado, 2019; Hardesty *et al.*, 2005; Pivello, 2011). In these areas, fire is considered an important element for nutrient cycling and for maintaining the diversity and structure of these ecosystems (Pausas and Bond, 2020; Pivello *et al.*, 2021). However, anthropogenic influence on fire regimes alters their frequency and seasonality patterns, posing a threat to the biodiversity conservation in these landscapes (Carvalho and Mustin, 2017; Oliveira *et al.*, 2022; Schmidt and Eloy, 2020).

To assess flora responses to fire, many studies combine controlled fire experiments with extensive in situ vegetation monitoring, as observed in studies carried out in savanna areas in Australia (Andersen *et al.*, 2003; Williams *et al.*, 2003), Africa (Higgins *et al.*, 2007; van Wilgen *et al.*, 2007) and also in the Cerrados of Brazil (Coutinho, 1990; Miranda, 2010). By providing detailed information about the flora before the fire and thoroughly monitoring the environmental characteristics during the fire (e.g., fire intensity, air temperature, wind speed, air humidity, etc.), the use of controlled fire experiments presents advantages over studies that rely on field information only after the fire has occurred (Furley *et al.*, 2008).

In addition to the use of information collected in-situ, the use of data derived from remote sensing has become an effective tool for monitoring the post-fire vegetation regeneration process (Gitas *et al.*, 2012; Pérez-Cabello *et al.*, 2021). It is worth highlighting the time series of the Landsat and Sentinel-2 satellite families. They have optical sensors that allow for the derivation of a series of spectral indices sensitive to the ecological dynamics of vegetation in different ecosystems (Harris *et al.*, 2011; Hill, 2013).

One of the most commonly used indices is the Normalized Difference Vegetation Index (NDVI) (Rouse *et al.*, 1974), which employs near-infrared and red spectral information to monitor the health of vegetation (Pettorelli *et al.*, 2005). It is commonly applied in studies aimed at assessing the impacts of events such as deforestation (Alves *et al.*, 2015; Fuentes *et al.*, 2024; Othman *et al.*, 2018) and wildfires (Chuvieco *et al.*, 2002; Morton *et al.*, 2011; Torres *et al.*, 2018). Regarding the analysis of burned areas, there are specific indices such as the Normalized Burned Ratio (NBR) (Key and Benson, 2006) and its variations, including NBR2 (Devries *et al.*, 2016) or NBR+ (Alcaras *et al.*, 2022). These differ from NDVI in that they integrate short-wave infrared spectral information. An important topic that combines the derivation of spectral indices and the analysis of fire effects refers to studies of spectral separability between burned and unburned areas, which contribute to the understanding of the detection and analysis of fire-affected areas (Lasaponara, 2006; Pacheco *et al.*, 2023). In optical remote sensing, spectral separability is defined as the ability to distinguish different types of objects or land uses and covers based on their reflectivity patterns across the electromagnetic spectrum (Rowan *et al.*, 2021).

The combination of data from Landsat and Sentinel-2 satellites has been increasingly used in the literature, based on the application of harmonization procedures (Berra *et al.*, 2024; Claverie *et al.*, 2017; Frantz, 2019; Nguyen *et al.*, 2020). The main advantage derived from this combination is that image acquisition is more frequently available. This helps overcome the challenges of the unavailability of cloud-free records in rainy regions, such as the Amazon (Asner, 2001; Roy *et al.*, 2006; Sano *et al.*, 2007). Furthermore, this increase in the number of multi-temporal records allows for more detailed monitoring of vegetation, which is especially important for tropical savannas, where the post-fire regeneration process is faster and more complex compared to other types of ecosystems (Alves *et al.*, 2018; Lhermitte *et al.*, 2011; Veraverbeke *et al.*, 2011). These characteristics are added to factors such as fire seasonality and fuel age (time since last fire), which influence the features of the fire and are fundamental to understanding its behavior and effects (Alves and Pérez-Cabello, 2017; Fontaine *et al.*, 2012; Pereira Júnior *et al.*, 2014).

This background led to the creation of the Campos Amazônicos Fire Experiment (CAFE) (Alves *et al.*, 2022), which was established to help understand the relationship between fire and flora in Amazonian savanna areas. At the same time, CAFE advanced the discussion about the ecological meaning of remote sensing derived datasets when compared with data obtained in the field. This is a study of experimental fire plots carried out using different seasonality and fire-return interval treatments on areas of open physiognomies of the largest savanna enclave of the southern Brazilian Amazon. The present work focuses on the evaluation of the dynamics of spectral separability and the post-fire vegetation recovery process of these experiments. This assessment is based on the use of a time series of harmonized images from Landsat and Sentinel-2 together with fuel loads accumulation data obtained in the field. Specifically, the aim is to: a) characterize the extent to which the combined use of Landsat and Sentinel-2 allows for an increase in the availability of cloud-free data in the time series; b) evaluate the effect of fire seasonality and fuel age on spectral separability using spectral indices; c) monitor the process of vegetation recovery after fire using spectral indices and a fuel load dataset obtained in the field. Therefore, the potential use of orbital remote sensing data is explored to better understand the effects and patterns of post-fire vegetation recovery on Amazonian savanna physiognomies, providing useful information for the territorial management process of these areas.

2. Methodology

2.1. Characteristics of the study area and experimental design

The study area is located in the middle of the largest enclave of predominance of open vegetation physiognomies in the southern Brazilian Amazon (Fig. 1), called Campos Amazônicos Savanna Enclave (CASE), which occupies a total of 4342 km² (Alves and Pérez-Cabello, 2017; ICMBio, 2016). The topography is marked by flat or gently undulating terrain, with dystrophic soils (neosols marked by the presence of plinthite in the B horizon) (ICMBio, 2016; Motta *et al.*, 2002). In terms of climate, the area has high average annual temperatures (≈24°C-28°C) and a seasonality marked by a strong concentration of precipitation between the months of October and April, which accounts for approximately 85% of the ≈2200 mm of annual precipitation (Marengo *et al.*, 2001). Between the months of May and September, there is an annual dry season, which coincides with a high number of fires in the area, mainly in the central and final months of this season (Alves and Pérez-Cabello, 2017).

In the context of CAFE, a total of 30 permanent monitoring plots were installed in 2019 in sectors of the enclave belonging to the Campos Amazônicos National Park (CANP), a conservation unit managed by the Chico Mendes Institute for Biodiversity Conservation that occupies approximately 47% of the total CASE area. Each plot was 1 hectare (100 x 100 m), and was divided according to different seasonality treatments (Early-Dry Season – EDS; or Middle-Dry Season – MDS fires) and fire-return intervals (biennial and triennial fires), which were defined randomly. The definition of seasonality is based on the classification of the annual dry season into three periods (Early-Dry Season, Middle-Dry Season and Late-Dry Season), where the first and last correspond to transition periods in relation to the rainy season. The central period includes the longest uninterrupted period of minimal rainfall during the dry season, usually occurring between the second half of July and the first half of September (Alves and Pérez-Cabello, 2017). The approaches that consider a dual division of the dry season (Early-Dry Season and Late-Dry season) can interpret the fire treatment of plots classified here as Middle-Dry Season as Late-Dry Season fires.

The analysis includes data related to 60 fire experiments conducted between 2019 and 2023 (Table 1). For the present study, the fire-return interval treatments were reclassified into three fuel age classes (time since last fire): i) 10-year-old or older fuel – including 24 fire experiments performed during 2019; ii) 2-year-old fuel – including 24 fire experiments carried out during 2021 and 2023; iii) 3-year-old fuel – including 12 fire experiments performed during 2022. All plot burning events were independent and carried out at similar times each day (closest to noon), and simulated the prevalent fire

behavior in open vegetation ecosystems using head fires (Cheney and Sullivan, 1997). Every fire trial was directly supervised by the CANP fire brigade to ensure safe burning (Alves *et al.*, 2022).

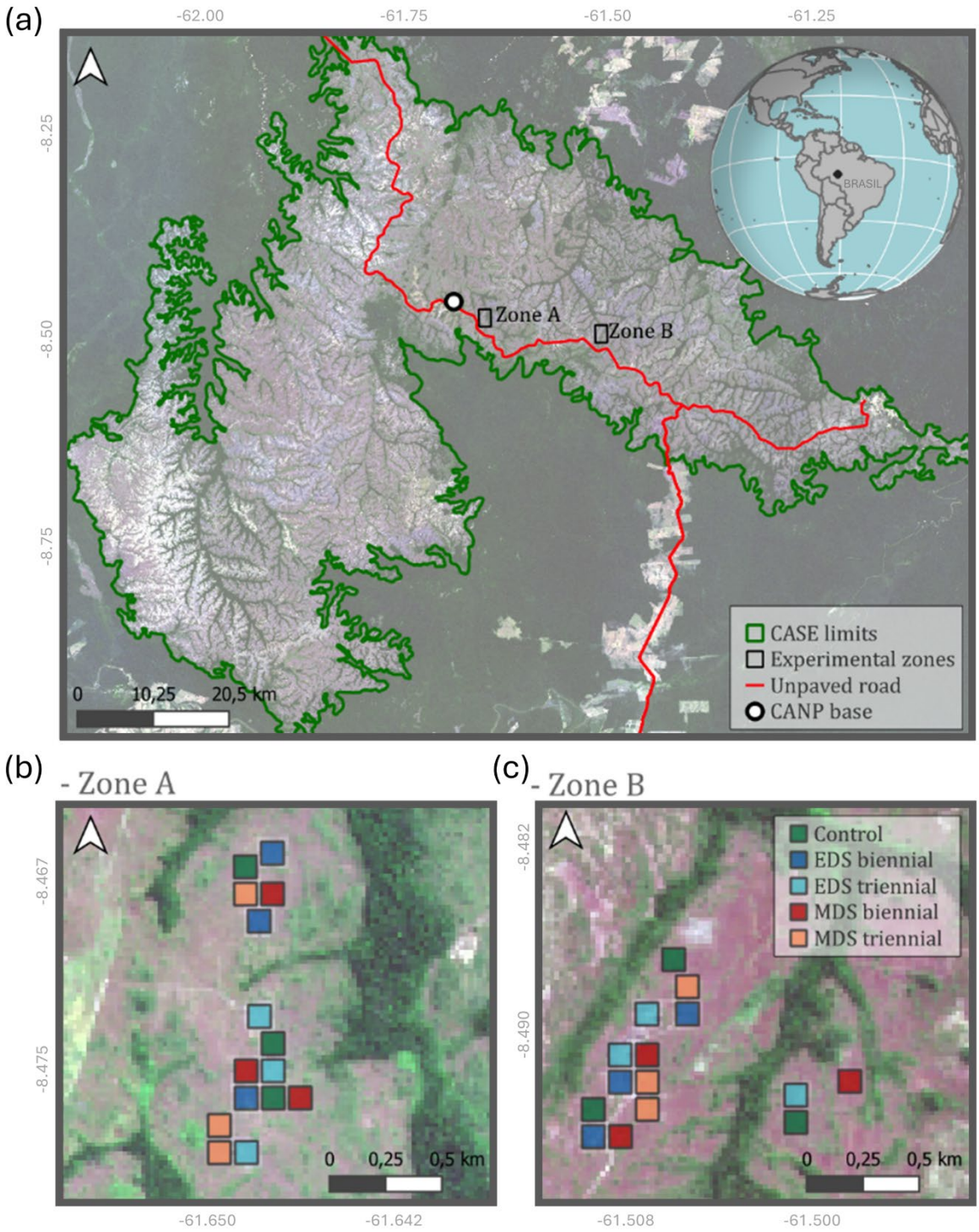

Figure 1. Location map of the study area (a) and the experimental plots in zones A (b) and B (c) of the Campos Amazônicos Fire Experiment (CAFE). In the background, in transparency, Landsat OLI image from August 16, 2023 on the upper map; and Sentinel-2 image from July 15, 2019 on the lower maps. EDS - Early-Dry Season; MDS - Middle-Dry Season; CASE – Campos Amazônicos Savanna Enclave; CANP – Campos Amazônicos National Park.

Table 1. Types of fire treatment carried out in each permanent monitoring plot of CAFE between 2019 and 2023. EDS - Early-Dry Season; MDS - Middle-Dry Season.

Plot	Fire season	Fire-return interval	Prescribed fire dates (yyyy/mm/dd)
A01	MDS fire	3 years	2019/08/25; 2022/09/06
A02	EDS fire	3 years	2019/05/21; 2022/05/25
A03	MDS fire	3 years	2019/08/25; 2022/09/06
A04	EDS fire	2 years	2019/05/25; 2021/05/27; 2023/06/03
A05	Control (unburned)	Control (unburned)	-
A06	MDS fire	2 years	2019/08/26; 2021/09/02; 2023/09/08
A07	MDS fire	2 years	2019/08/26; 2021/09/02; 2023/09/09
A08	EDS fire	3 years	2019/05/21; 2022/05/26
A09	Control (unburned)	Control (unburned)	-
A10	EDS fire	3 years	2019/05/19; 2022/05/26
A11	EDS fire	2 years	2019/05/25; 2021/05/27; 2023/05/31
A12	MDS fire	3 years	2019/08/26;2022/09/07
A13	MDS fire	2 years	2019/08/26; 2021/09/01; 2023/09/09
A14	Control (unburned)	Control (unburned)	-
A15	EDS fire	2 years	2019/05/25; 2021/05/23; 2023/06/02
B01	EDS fire	2 years	2019/05/22; 2021/05/26; 2023/05/30
B02	MDS fire	2 years	2019/08/22; 2021/08/28; 2023/09/06
B03	Control (unburned)	Control (unburned)	-
B04	MDS fire	3 years	2019/08/23; 2022/09/05
B05	EDS fire	2 years	2019/05/23; 2021/05/25; 2023/05/30
B06	MDS fire	3 years	2019/08/23; 2022/09/04
B07	EDS fire	3 years	2019/05/23; 2022/05/24
B08	MDS fire	2 years	2019/08/24; 2021/08/28; 2023/09/07
B09	EDS fire	3 years	2019/05/23; 2022/05/24
B10	EDS fire	2 years	2019/05/24; 2021/05/25; 2023/05/30
B11	MDS fire	3 years	2019/08/24; 2022/09/03
B12	Control (unburned)	Control (unburned)	-
B13	Control (unburned)	Control (unburned)	-
B14	EDS fire	3 years	2019/05/24; 2022/05/23
B15	MDS fire	2 years	2019/08/22; 2021/08/27; 2023/09/07

The plots were divided into two permanent monitoring zones (Zones A and B) and met the following criteria regarding their areas, which were: (i) representative of the dominant open savanna vegetation that is characteristic of the region (grasses with scattered shrubs and low tree density); (ii) not affected by invasive species; (iii) not influenced by recent fires, i.e., absence of fire for at least 10 years; (iv) contiguous homogeneous areas able to accommodate a reasonable number of replicate plots, and (v) in close proximity to the CANP main base station, as these were remote areas with difficult access (Alves *et al.*, 2022). All plots were established in areas with less than 20% tree cover (and avoiding tree clumps), on slopes shallower than 5°, and at least 20 meters from each other. Additionally, each plot was precisely placed to provide the best alignment with the pixel grids of the Sentinel-2 and Landsat satellites (covering exactly 25 full Sentinel-2 pixels and 9 full Landsat pixels) (Alves *et al.*, 2022).

2.2. Processing of remote sensing data

The study uses time series from the optical sensors on the Landsat and Sentinel-2 satellite families. These series underwent harmonization procedures in order to ensure greater availability of information free from the effects of clouds and other atmospheric disturbances. In terms of the analyzed time window, all images were processed between 2019 and 2023, totaling five years of monitoring the different fire treatments.

The following image collections were used as input data: Collection 2 calibrated top-of-atmosphere (TOA) reflectance derived from the Landsat 7 and Landsat 8 satellites sensors (Enhanced Thematic Mapper Plus - ETM+, and Operational Land Imager - OLI, respectively); and Level-1C orthorectified TOA reflectance from the Sentinel-2A and Sentinel-2B (both equipped with a MultiSpectral Instrument-MSI sensor). These collections underwent different correction procedures to complete the harmonization process, based on a set of codifications programmed in a Jupyter Notebook environment (JT, 2015) and Google Earth Engine (GEE) (Gorelick *et al.*, 2017), through the adaptation and integration of free codes available in the literature (Fig. 2).

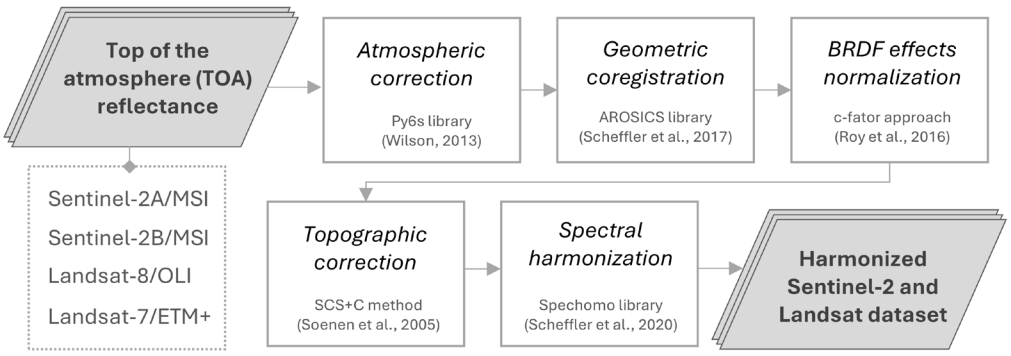

Figure 2. Processing steps for harmonizing the datasets used.

The procedures generally follow those previously applied by Alves *et al.* (2022) for the evaluation of the spectral separability in selected immediate post-fire records from experimental fires carried out during 2019. In addition to expanding the time window of analysis in relation to the previous study, this work also uses the most recent Landsat collection (Collection 2), and includes topographic correction processes. Each of the procedures performed is detailed below:

- *Atmospheric correction*: The TOA images were initially subjected to an atmospheric correction process using a common algorithm for Landsat and Sentinel-2 sensors, through a 6S radiative transfer model implemented in a Py6s Python API (Wilson, 2013). The application was encoded based on the freely available scripts of Nguyen *et al.* (2020), which in turn adapt a version encoded and offered by Murphy (2020). As a result, the Bottom of Atmosphere (BOA) reflectance data (also known as surface reflectance) of each collection were obtained.
- *Geometric coregistration*: a spatial coregistration was implemented using an Automated and Robust Open-Source Image Co-Registration Software (AROSICS) Python API (Scheffler *et al.*, 2017), which was encoded based on API documentation (http://danschef.gitext.gfz-potsdam.de/arosics/doc/index.html). The co-registration process was carried out according to a phase correlation for sub-pixel shift estimation and reproduced using the cloud-free Landsat record as a reference. This record presents the smallest geometric root mean square error according to the data producer.
- *Bidirectional Reflectance Distribution Function (BRDF) normalization*: the BRDF effects were computed and corrected based on the general method developed by Roy *et al.* (2016) for Landsat data using the c-factor approach. This method was also successfully applied over Sentinel-2 datasets. The correction was performed by applying properly calibrated and band-tested coefficients to adjust the viewing angle of the images, resulting in the nadir BRDF-adjusted BOA data. BRDF normalization was implemented within the GEE platform and also encoded based on the freely available scripts Nguyen *et al.* (2020).

- *Topographic correction*: to reduce the influence of terrain slope and aspect on the spectral signal, a topographic correction was implemented using the sun-canopy-sensor with a semi empirical moderator (SCS+C) method (Soenen *et al.*, 2005), which was encoded based on the freely available scripts of Nguyen *et al.* (2020) and Poortinga *et al.* (2019) in GEE. To obtain the elevation and terrain slope parameters required for model reproduction, the Copernicus Global 30 meters Digital Elevation Model (DEM) (ESA, 2024) was used.
- *Band pass adjustment*: spectral harmonization was processed using the SpecHomo Python library (Scheffler *et al.*, 2020). SpecHomo offers different machine learning techniques for the prediction of the target sensor spectral information. It employs the Landsat 8 band spectral resolution (OLI) as the target sensor and applies the linear regressions with 50 clusters based on the best results obtained in tests conducted by library producers (Scheffler *et al.*, 2020). The processing was carried out by developing a script based on the documentation provided by the authors (https://github.com/GFZ/spechomo).

In order to complete the harmonization, 'nodata' masks were applied to pixels affected by cloud or cloud-shadows, and all images were reprojected into the same coordinate reference system (WGS 84/UTM 20S). Also, Sentinel-2 images were resampled to the 30 meters of spatial resolution of Landsat pixel grid using an area-weighted average. For specific cases where more than one cloud-free record existed for the same date (related to specific dates of overlapping surveys between Landsat and Sentinel-2), the defined criterion was to prioritize the original Landsat 8 records over all other information, since it was the target sensor in the series. For cases where Sentinel-2 and Landsat 7 data overlapped, the information related to the former was given priority.

The resulting harmonized series provided full 9 pixels for each plot intended to spectrally match four specific bands of Landsat 8 OLI: red, near infrared (NIR), and short-wave infrared bands ($SWIR_1$ and $SWIR_2$), considering the band correspondence available on Table 2. The order of implementation of the applied correction types follows the same flow defined by Claverie *et al.* (2017) in the Harmonized Landsat and Sentinel-2 (HLS) product of the National Aeronautics and Space Administration (NASA). The development of a specific harmonization routine in the context of the present study is explained by the fact that the HLS/NASA product neither integrates Landsat 7 (ETM+) images as input data, nor maintains the original pixel alignment of the TOA images in its final product.

Table 2. Correspondence between Sentinel 2 (MSI sensor) and Landsat (ETM+ and OLI) spectral bands used in the present study.

Spectral band	**Sentinel 2A**		**Sentinel 2B**		**Landsat ETM+**		**Landsat OLI**	
	Band	Bandwidth (μm)	Band	Bandwidth (μm)	Band	Bandwidth (μm)	Band	Bandwidth (μm)
Red	4	0.65 - 0.68	4	0.65 - 0.68	3	0.63 - 0.69	4	0.63 - 0.69
NIR	8	0.78 - 0.89	8	0.78 - 0.89	4	0.77 - 0.90	5	0.77 - 0.90
$SWIR_1$	11	1.57 - 1.66	11	1.56 - 1.66	5	1.55 - 1.75	6	1.55 - 1.75
$SWIR_2$	12	2.11 - 2.29	12	2.09 - 2.28	7	2.09 - 2.35	7	2.09 - 2.35

Based on the harmonized surface reflectance series, a time series of the spectral indices NDVI (Eq. 1) and NBR2 (Eq. 2) was derived, according to the formulas below, where ρ represents the reflectance value of the spectral band:

$$\mathrm{NDVI} = \frac{\rho_{\mathrm{NIR}} - \rho_{\mathrm{Red}}}{\rho_{\mathrm{NIR}} + \rho_{\mathrm{Red}}} \quad \text{(Eq. 1)}$$

$$\mathrm{NBR2} = \frac{\rho_{\mathrm{SWIR_1}} - \rho_{\mathrm{SWIR_2}}}{\rho_{\mathrm{SWIR_1}} + \rho_{\mathrm{SWIR_2}}} \quad \text{(Eq. 2)}$$

The choice of NDVI is associated with its potential to monitor the health status of vegetation (Pettorelli *et al.*, 2005). On the other hand, NBR2 was selected due to its high performance of spectral separability between burned areas in different fire seasons, as proven in a previous study on the immediate effects of fire carried out on part of the sample universe analyzed in the present study (Alves *et al.*, 2022).

2.3. Collection and processing of field data

Although the CAFE context involves a larger universe of data monitored in the field, in the present study biomass accumulation measures are evaluated as a proxy to understand vegetation cover recovery processes compared to data observed by satellite sensors. Measurements of fine fuel load (above ground biomass) were obtained from 8 samples of 0.5 × 0.5 m randomly distributed within each plot. The samples included graminoids, leaves, and branches near the ground (Fig. 3). Fresh biomass was dried at 70°C for 48 hours and weighed, resulting in a total fine fuel load (kg. m^{-2}) measure for each sample (Miranda *et al.*, 1996; Rissi *et al.*, 2017). Additionally, the consumed fuel load (kg. m^{-2}) was calculated by subtracting the total fine fuel load before and just after fire.

Since 2019, two annual fine fuel load collection campaigns have been carried out across all plots. The first one took place in the initial months of the annual dry season (May or early June) and the second in the transition from the central months to the end of the annual dry season (late August/early September). When a plot underwent a fire treatment during a given collection window, data from before and after the application of fire were generated. For the present study, the analysis includes data obtained in 10 collection campaigns (May 2019; August 2019, May 2020; August 2020; June 2021; September 2021; May 2022; September 2022; May 2023; September 2023), each of which lasted approximately 6 days.

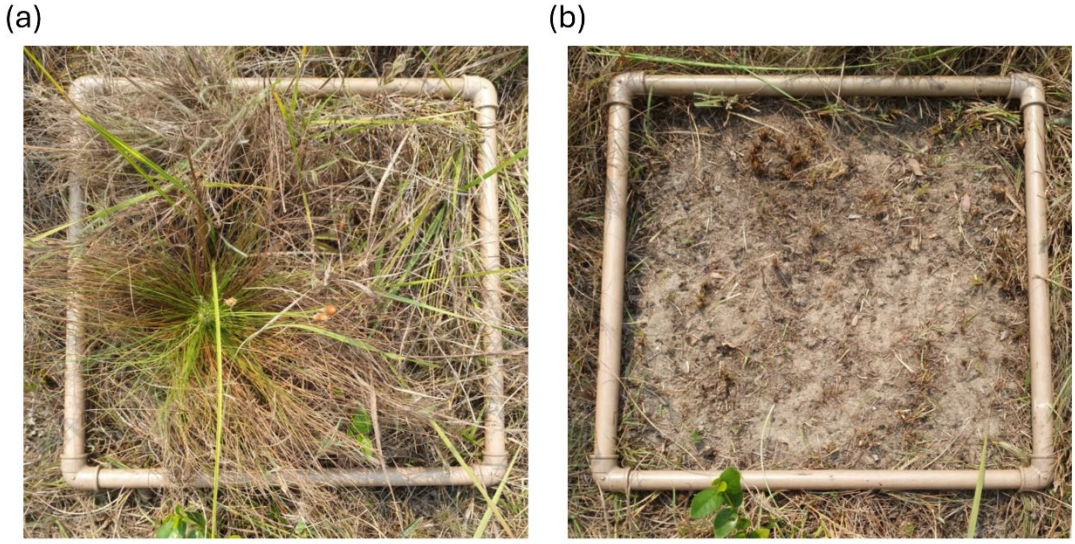

Figure 3. Example of a fine fuel load sample of 0.5 × 0.5 m collected in the field campaigns: before (a) and after (b) collection.

2.4. Data analysis

First, an evaluation of the generated harmonized series was carried out. For this purpose, specific records were used where the date of Landsat and Sentinel-2 cloud-free imaging coincided (a total of 13 imaging dates). A Pearson correlation statistic (r) between the harmonized Sentinel-2 and Landsat data was generated, along with the extraction of its p-values, both for the NDVI and NBR2 data. It was also evaluated to what extent the combined use of Landsat and Sentinel-2 data increased the availability of cloud-free or partially cloud-free images compared to the use of the individual series.

Then, the temporal trajectories of each spectral index were grouped by each fire treatment and plotted using the 'ggplot 2' package within the R software (RCT, 2019). For the visual arrangement of the temporal trajectories of the spectral indices, the DATimeS toolbox (Belda *et al.*, 2020) was used in order to generate a continuous series of data. This offered multiple algorithms to fill gaps of time series data. The NDVI and NBR2 series were processed using the shape-preserving piecewise cubic interpolation algorithm (Fritsch and Carlson, 1980). This algorithm avoided excessive smoothing of data in situations of abrupt changes in the time series. It was used in combination with a Savitzky-Golay filter (span = 7; degree = 2) to provide a continuous record every five days in the period from 2019 to 2023 for each fire treatment carried out. To assist in visualizing the seasonality of the area, daily precipitation data derived from the Climate Hazards Center InfraRed Precipitation with Station data (CHIRPS) product (Funk *et al.*, 2015) were extracted and plotted together with the generated indices time series.

In addition to the visual assessment of changes in trajectories, statistics were extracted to understand the spectral separability of each index in the face of fire occurrences, grouping the plots according to seasonality and time since the last fire treatments. To this end, the mean absolute difference between the burned and unburned values in the immediate post-fire conditions of each plot was extracted and compared between the groups. Furthermore, M-Statistics was used, a statistic widely employed to analyze spectral differences in fire-affected areas that quantifies "histogram separation" based on the mean and standard deviation relations (Fornacca *et al.*, 2018; Kaufman and Remer, 1994; Pacheco *et al.*, 2023). Values of M-Statistics greater than 1 suggest good spectral separability between groups (Kaufman and Remer, 1994). These statistics were further compared with consumed fuel load values, exploring the correspondence between spectral and field values through correlation analysis. The two-way Analysis of Variance (ANOVA) ($p < 0.05$) and Post-hoc Tukey ($p < 0.05$) tests were also performed to evaluate whether or not there were statistically significant differences between fire treatment groups. Only results that passed the normality (Kolmogorov-Smirnov test, $p > 0.05$) and homoscedasticity (Levene's test, $p > 0.05$) tests were considered in the analysis.

Finally, to assess the vegetation recovery process after the fire, we focused on analyzing the time period from 2019 to 2022, considering the plots burned during 2019. This time frame offered a longer time window of post-fire information without the effects of a second fire on the same plot, allowing us to evaluate the variation in pre-fire conditions, immediate post-fire conditions, and one to three years after fire. Therefore, M-Statistics spectral separability calculations were generated for records up to three years after the fire and analyzed together with fine fuel load accumulation to evaluate the vegetation recovery process.

3. Results

3.1. Evaluation of the generated harmonized time series of spectral indices

Of the total of 488 images available from all sensors in the period from 2019 to 2023, only 40.16% were considered relevant, as they provided information that was partially or totally free of clouds, cloud shadow, or other atmospheric disturbance effects. Of this total, 74 belonged to the Landsat series (OLI = 52; ETM+ = 22), and another 122 to the Sentinel-2 series (2A/MSI = 66; 2B/MSI = 56). In other words, the combined use of Landsat and Sentinel 2 provided an increase of 62.81% in cloud-free or partially cloud-free images when compared to the exclusive use of the Landsat series, or 38.69% in relation to the exclusive use of the Sentinel-2 series.

Based on the comparison of specific records in which the Landsat and Sentinel-2 imagery dates coincide, it was possible to evaluate the consistency of the generated harmonized product. High levels of correlation were observed for both the NDVI values ($r = 0.912$; $p < 0.01$) and the NBR2 index ($r = 0.948$; $p < 0.01$) (Fig. 4).

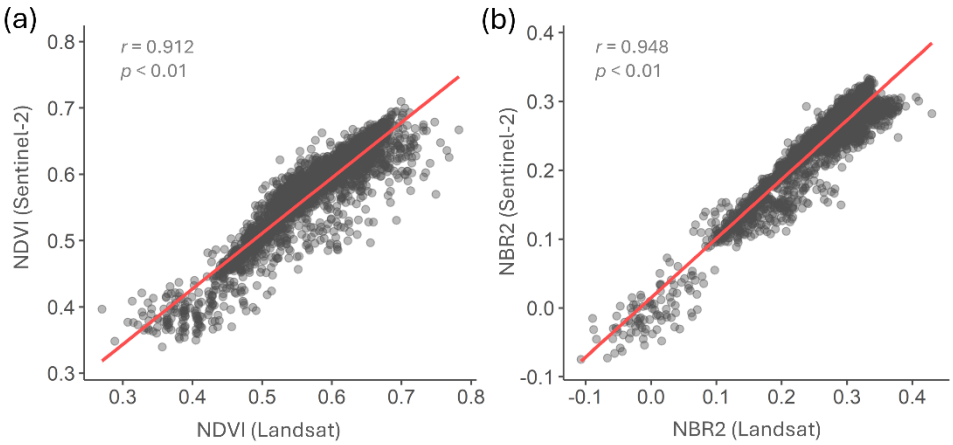

Figure 4. Scatterplots comparing harmonized Landsat and Sentinel-2 NDVI (a) and NBR2 (b) values (n = 2561), considering data from coincident imaging dates between the series in the period from 2019 to 2023.

3.2. Spectral separability and dynamics of vegetation recovery after fire

The different fire treatments applied reflected marked variations in the trajectories of the harmonized NDVI (Fig. 5) and NBR2 (Fig. 6) series. In both indices, the control plots (fire-excluded) presented an annual cycle of decreasing values associated with the effects of water stress during the dry months, which were slightly more pronounced in the NDVI values compared to the NBR2 index. On the other hand, it was observed that the plots treated with fire, regardless of the variation in the type of treatment, generated abrupt drops in the NDVI and NBR2 values as an immediate effect of the burning.

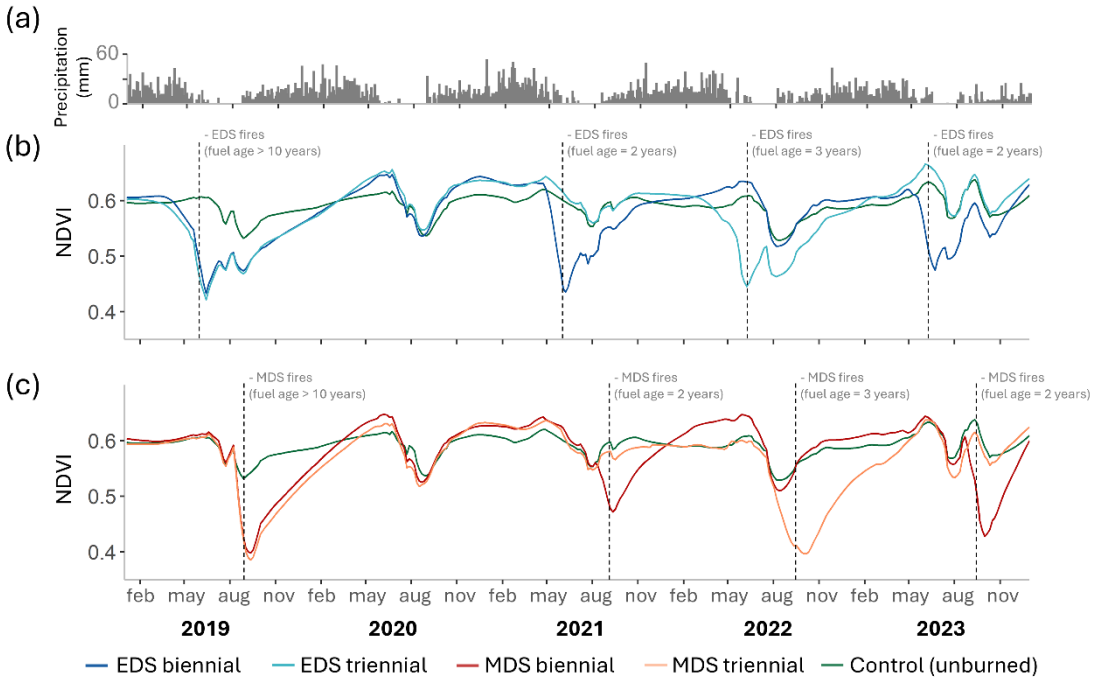

Figure 5. NDVI harmonized time series from 2019 to 2023 grouped by EDS (Early-Dry Season) fires (b) and MDS (Middle-Dry Season) fires (c) fire treatments versus control plots. Daily precipitation (a) is also shown as auxiliary information based on a CHIRPS dataset.

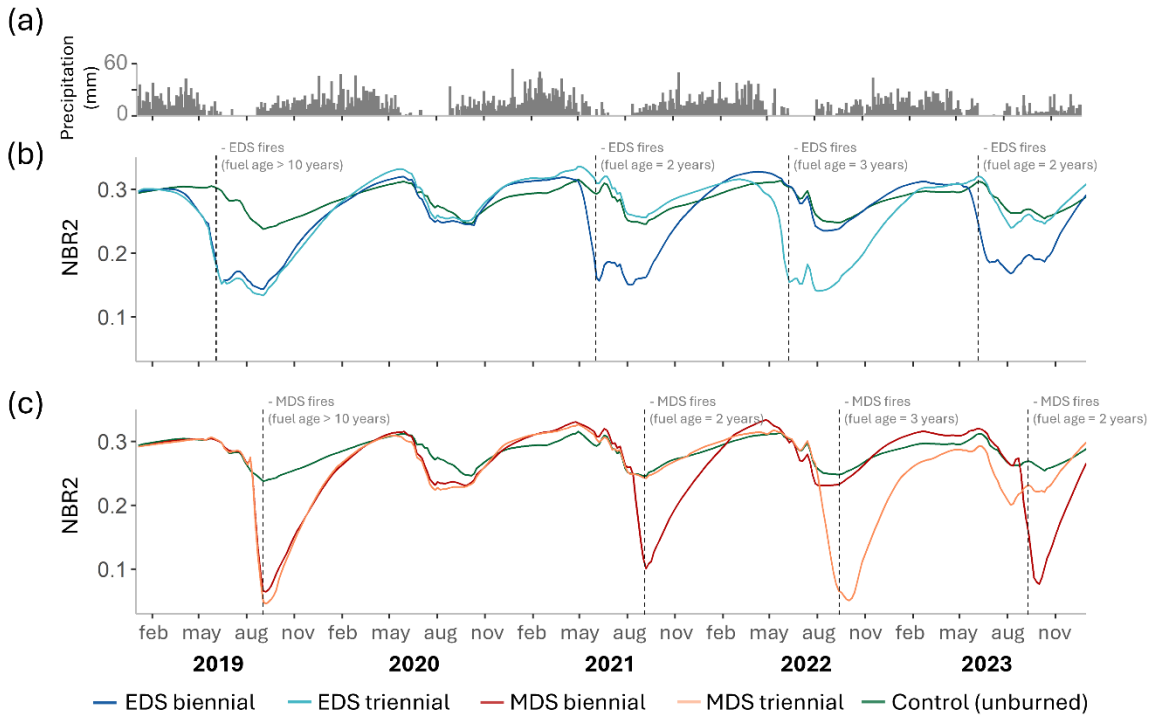

Figure 6. NBR2 harmonized time series from 2019 to 2023 grouped by EDS (Early-Dry Season) fires (b) and MDS (Middle-Dry Season) fires (c) fire treatments versus control plots. Daily precipitation (a) is also shown as auxiliary information, based on a CHIRPS dataset.

These visual differences in the immediate effects of fire for all fire treatments were observed in high spectral separability values for both indices (M-statistics mean ± standard error of 8.773 ± 2.200 for NDVI; and 8.866 ± 1.321 for NBR2) (Table 3). When comparing the mean absolute difference (burned – control plot values), the two-way ANOVA test revealed statistically significant differences between the fire treatment groups for the NBR2 index only in relation to both seasonality groups ($F = 81.550$; $p = 7.74 \cdot 10^{-12}$) and time since last fire ($F = 15.205$; $p = 8.08 \cdot 10^{-6}$).

Table 3. Spectral responses of the NDVI and NBR2 indices to different seasonality and fuel age treatments in terms of mean absolute difference (burned – control) and M-Statistics, as well as their respective mean values of consumed fuel loads recorded in the field. EDS - Early-Dry Season; MDS - Middle-Dry Season.

Season	Time since last fire (fuel age)	NDVI		NBR2		Consumed fuel load (kg. m^{-2})
		Mean absolute difference	M-Statics	Mean absolute difference	M-Statics	
EDS	≥ 10 years	0.144	4.628	0.147	4.955	0.525
EDS	3 years	0.203	8.796	0.161	9.008	0.618
EDS	2 years	0.148	5.157	0.116	6.283	0.431
MDS	≥ 10 years	0.159	5.867	0.235	9.947	0.760
MDS	3 years	0.157	19.092	0.213	14.266	0.720
MDS	2 years	0.148	9.099	0.175	8.737	0.546
Average		0.160	8.773	0.174	8.866	0.600
Sd		0.022	5.391	0.043	3.235	0.124

NBR2 presented a pattern of abrupt drops in its values. On average they were 66.34% higher for MDS fires than for EDS fires (0.208 mean values for MDS fires versus 0.138 for EDS fires). Among the time since last fire treatments, the results of the Tukey HSD test revealed that the drops in NBR2 values in the burned areas with a fuel age of two years (0.147 mean values) were significantly smaller than those observed in the areas with a fuel age of 3 and 10 years (0.194 and 0.191 values, respectively). The mean absolute difference values of NBR2 also showed a strong correlation with the consumed fuel load data obtained in the field (r = 0.646). This contrasts greatly with the same analysis carried out in relation to the NDVI data (r = 0.032).

Focusing on the time frame between 2019 and 2022 for the EDS and MDS triennial treatments helps assess the vegetation recovery process from fire. In the multitemporal trajectories of the NDVI and NBR2 indices (Fig. 5 and Fig. 6), it was observed that after registering abrupt drops in their values in response to the immediate effects of fire in 2019, these areas underwent a gradual greening up process in the remainder of the year, which continued until approximately the end of the rainy season of the following year.

The beginning of the dry season of the year following the fire is marked by values that sometimes even exceed those observed in fire-excluded plots, especially in the NDVI index. This situation was observed in the months of May and June 2020, in response to the fire experiments reproduced in 2019, and was again noticeable in the same months of 2022 in response to the fire experiments reproduced in 2021. Throughout the dry season of the year following the fire, the burned plots again presented lower values than the unburned plots, a fact observed with greater magnitude in the NBR2 values of the MDS fires. After two years, such differences were no longer clearly noticeable.

This pattern of vegetation recovery described from the index trajectories was visualized both in the spectral separability assessment (M-Statistics) and in the data on the fine fuel loads accumulation in the three years following the fire (Table 4). In terms of M-Statistics, after presenting consistently high values in the immediate post-fire period in 2019 (ranging from 4.628 to 9.947), values greater that 1 were only observed at the end of the dry season of the year following the fire. This denotes good spectral separability, especially in the NBR2 values.

Table 4. Temporal variation of spectral separability (M-Statistics) based on the evaluation of data from the years following the experiments carried out in 2019, accompanied by the values corresponding to the accumulation of fine fuel loads. EDS - Early-Dry Season; MDS - Middle-Dry Season.

Year	**Month and day**	**NDVI M-statistics**		**NBR2 M-statistics**		**Fine fuel load accumulation (kg. m^{-2})**	
		EDS	MDS	EDS	MDS	EDS	MDS
2019 (pre- and immediate postfire)	May 17	0.011	0,033	0.098	0.083	0.727	0.736
	*	4.628	5.867	4.955	9.947	0.190	0.048
2020 (after 1 rainy season)	May 27	0.893	0.176	0.234	0.290	0.453	0.420
	Aug 23	0.026	1.097	1.418	3.283	0.496	0.441
2021 (after 2 rainy seasons)	April 28	0.077	0.061	0.610	0.472	0.609	0.601
	Aug 18	0.350	0.313	0.492	0.014	0.628	0.657
2022 (after 3 rainy seasons)	May 10	0.046	0.065	0.046	0.065	0.780	0.797
	Aug 13	**	0.304	**	0.077	**	0.798

*May 25 for EDS; and Aug 29 for MDS fires; ** values not considered as the plots underwent a new fire at June 2022.

The variation in the fine fuel accumulation data (Table 4) is consistent with the rapid recovery process depicted by the spectral indices. Once a rainy season had passed after the application of fire treatments, an average recovery of 48.98% and 54.07% of the fine fuel consumed by the EDS and MDS

fires, respectively, was recorded. After two years, at the beginning of the dry season of 2021, this recovery reached 78.02% for EDS and 80.38% for MDS fires. Finally, at the beginning of the dry season of 2022 (three rainy seasons after the fire), this recovery already reached a level similar to, and even slightly higher than, the fine fuel accumulation conditions observed before the fire. Figure 7 exemplifies the comparisons made in Table 3, helping to understand the vegetation recovery process. It is noteworthy that, despite the differences in the fuel loads consumed in immediate EDS and MDS post-fire situations, both treatments reached fine fuel accumulation values similar to those observed in pre-fire conditions three rainy seasons after the fire.

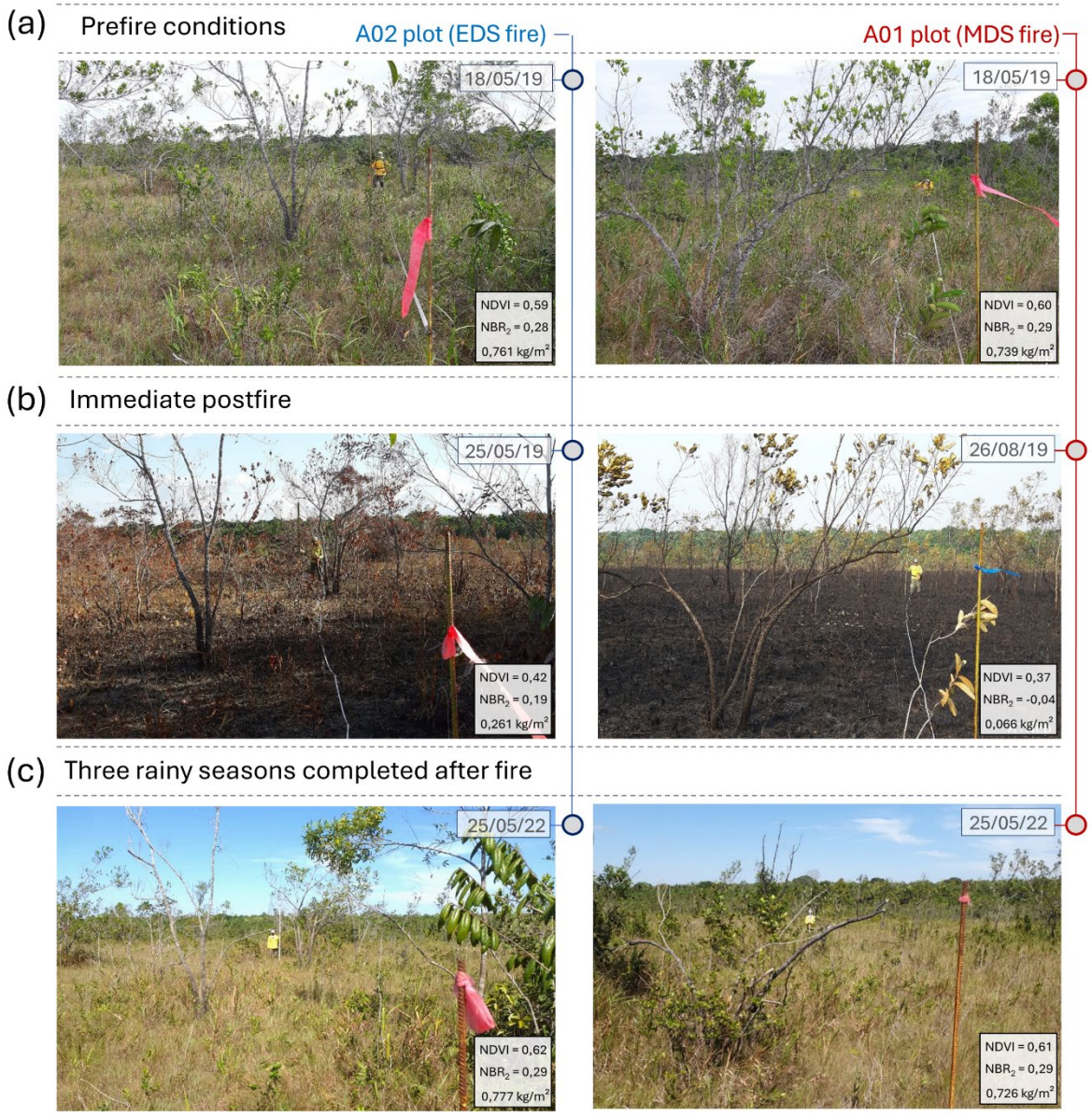

Figure 7. Vegetation dynamics comparing pre-fire (b), immediate post-fire (b), and three rainy seasons completed after fire (c) in sectors of A02 (Early-Dry Season - EDS triennial fire) and A01 (Middle-Dry Season - MDS triennial fire) plots. Each photograph includes the date, the average NDVI and NBR2 values, as well as the total fine fuel load observed in the aforementioned plot.

4. Discussion

The generation of a time series of spectral indices from harmonization processes ensured a significant increase in the availability of images used, namely 62.81% in relation to the exclusive use of the Landsat series, or 38.69% in the case of the Sentinel-2 series. These results were consistent with those observed by Bolognesi *et al.* (2020), who indicated that the inclusion of Landsat 8 data increased the number of images available by more than 40% compared to the exclusive use of Sentinel-2 images. The proportion of cloud-free images found here also matches that discussed by Claverie *et al.* (2018), who indicated that using the HLS/NASA dataset increased the availability of cloud-free images by 30-50% compared to using one dataset alone. In terms of verifying the quality of the series, the comparison of the specific records in which the Landsat and Sentinel-2 imagery dates coincided revealed high levels of correlation for both NDVI (r = 0.91) and NBR2 (r = 0.95) values. When assessing spectral correspondence between Landsat 8 and HLS/NASA, Wulder *et al.* (2021) found correlation levels ranging from 0.85 to 0.92 for spectral channels and r = 0.94 for NBR.

Based on the harmonized time series, it was possible to advance discussions on spectral separability between burned and unburned areas in open savanna vegetation ecosystems of the Brazilian Amazon. This study improves a previous one that focused on evaluating the effects of fire seasonality in immediate post-fire conditions (Alves *et al.*, 2022). More precisely, in addition to reinforcing the role of fire seasonality using a much larger dataset of experimental fires (60 versus 24 that were previously evaluated), the importance of the time since last fire (fuel age) variable for the spectral separability of fire was also proven.

Regarding seasonality, the mean absolute difference NBR2 values showed abrupt drops that were 66.34% higher for MDS fires than for EDS fires. This is largely explained by the fact that EDS fires are generally cooler and less intense in comparison with MDS fires (Alves *et al.*, 2022; Andersen *et al.*, 2003; Rissi *et al.*, 2017), generating different levels of consumed fuel loads.

In the evaluation of spectral separability between different fire treatments of fuel age, areas with 2-year-old fuels presented mean absolute difference NBR2 values with statistically significant differences in relation to areas with 3 or 10-year-old or older fuels. The fine fuel load accumulation data collected in the present study helped interpret this information: 3-years-after-the-fire areas reached fine fuel accumulation levels already similar to those observed in plots that had been free of fire for 10 years or more. The importance of fuel age is demonstrated in studies such as that of Halsey *et al.* (2009) in chaparral ecosystems, where 3-year-old fuel age is associated with fire spread conditions under moderate weather. In an analysis of tropical savanna ecosystems in Australia, Collins *et al.* (2023) found that areas treated with fire to reduce fuel three to five years ago were already likely to experience high-severity fires under critical drought conditions. Unlike NBR2, NDVI was not specifically designed to understand burned areas, but rather the state of vegetation in general, which may explain its worse performance in comparing spectral separability between the different fire treatments.

These results reinforce the potential of combined use of the Landsat and Sentinel-2 time series to provide a denser and spectrally consistent time series, assisting to overcome the challenges of the unavailability of cloud-free records in rainy regions, such as the Amazon (Sano *et al.*, 2007). Although the results focused on the evaluation of Amazonian savanna areas, our bespoke approach to harmonizing Landsat and Sentinel-2 can be applied to assess the effects of fire on different types of ecosystems, and is especially valid for monitoring areas strongly influenced by seasonality, such as other tropical savannas and grasslands landscapes across the globe. However, limitations in using this harmonized series may still occur for studies that require more detailed information during the rainiest months of the year, such as specific applications related to understanding the phenological dynamics of certain groups of plants. In these cases, from the point of view of optical remote sensing applications, there are other alternatives such as carrying out systematic imaging using multitemporal sensors on Unmanned Aerial Vehicles (UAVs) (Pineda Valles *et al.*, 2023), or even through the installation of terrestrial digital cameras (phenocams) for daily monitoring of plant dynamics in specific areas (Alberton *et al.*, 2017).

Such alternatives can provide even greater levels of detail than those presented in this study, generating information with greater spatial and temporal resolution that allows for the analysis of more specific targets associated with the monitoring of fire-affected areas.

When assessing the vegetation recovery process, it could be seen that the fire scar signal observed immediately after the fire gradually recovered in the following years. After three rainy seasons, its effects were no longer noticeable in terms of vegetation indices or data on the accumulation of fine fuel loads. The areas analyzed reflected, in general terms, a pattern observed in other grassland and savanna areas of the world, where recovery occurs three years after the fire (Bousquet *et al.*, 2022). Regarding the combustible material data, the results achieved are similar to those observed by Oliveira *et al.* (2021) who found that post-fire recovery of fuel loads takes, on average, 2.43 years.

However, it is important to note that the recovery of the vegetation evaluated here largely reflects the responses of the herbaceous layer, which is dominant in the Amazonian savanna physiognomies assessed. Although woody species occupy a reduced space in these areas, the effects of different fire treatments can result in various levels of mortality and treetop kill, affecting the dynamics of plant regeneration and the diversity of species in the area (Hoffmann *et al.*, 2009). Still in relation to the herbaceous layer, Laurentino (2023) recorded an increase in species diversity in burned areas with 2-year-old fuel age compared to areas with 10- or more years-old fuel age, regardless of fire seasonality, using the same sample universe as the present study. Such factors observed in tree species and at the species level of the herbaceous stratum may help to explain the higher NDVI values (see Fig. 5) up to two years after fire compared to unburned areas.

5. Conclusions

This study reinforces the potential of using harmonized multitemporal Landsat and Sentinel-2 series for the analysis of spectral separability and the vegetation recovery process in Amazonian savannah environments. The combined use of Sentinel-2 and Landsat resulted in an availability of cloud-free or partially cloud free images ≈0.6 times greater than that obtained with the exclusive use of Landsat images, ensuring a more detailed reading of the multitemporal variation of spectral indices related to vegetation responses to fire.

In the spectral separability analyses associated with the different fire seasonality and fuel age treatments, the potential of the NBR2 index stood out, as it responded with statistically significant differences both when comparing the groups of EDS and MDS fires and when comparing areas with 2-year-old fuel to those with 3-year-old fuel or more than 10-year-old fuel age. The same index also showed a strong correlation with the data on the consumed fine fuel load, highlighting its potential as an indicator of fire severity in open ecosystems of Amazonian savannahs.

Spectral information from satellites and field data converged in detecting a rapid vegetation response to fire in these ecosystems. This demonstrates that, three rainy seasons after the fire, conditions are similar to those observed before it. In summary, the results of this study reinforce the potential use of remote sensing data in the assessment of fire-affected areas in Amazonian savannah environments, exploring the ecological meaning and the connections between field and satellite data.

Acknowledgements

We thank the *Fundação Cearense de Apoio ao Desenvolvimento Científico e Tecnológico* (FUNCAP, process number BP6-00241-00158.01.00/25) as a research productivity fellowship provided for the first author; the Ministerio de Ciencia e Innovación/Agencia Estatal de Investigación de España (Grant No. PID2020-118886RB-I00); the Fundação de Amparo à Pesquisa do Estado de São Paulo (FAPESP, grant number 2019/07357-8) and the Conselho Nacional de Pesquisa e Desenvolvimento (CNPQ, processes number 441968/2018-0 and 154660/2018-3), that supports the initial years of the

project. We are also grateful to all the team of Laboratory of Vegetation Ecology (LEVeg) of the São Paulo State University, headed by Dr. Alessandra Fidelis, that supports fuel load data collections and fire behavior monitoring; and to the management team of the CANP, and in particular to its Fire Brigade (squad leaders José Furtado Neto, Genaldo Júnior, Ademilton Carvalho, Simei Limoeiro, Antonio Machado and Leandro Lacerda, and on behalf of them to all other members of the brigade).

Referencias

Ab'Saber, A., 1977. Espaços ocupados pela expansão dos climas secos na América do Sul, por ocasião dos períodos glaciais quaternários. *Paleoclimas* 3, 1-19.

Ab'Saber, A.N., 2003. *Os domínios de natureza no Brasil*: potencialidades paisagísticas. Ateliê Editorial, São Paulo.

Alberton, B., Torres, R. da S., Cancian, L.F., Borges, B.D., Almeida, J., Mariano, G.C., Santos, J. dos, Morellato, L.P.C., 2017. Introducing digital cameras to monitor plant phenology in the tropics: applications for conservation. *Perspectives in Ecology and Conservation* 15, 82-90. https://doi.org/10.1016/j.pecon.2017.06.004

Alcaras, E., Costantino, D., Guastaferro, F., Parente, C., Pepe, M., 2022. Normalized Burn Ratio Plus (NBR+): A New Index for Sentinel-2 Imagery. *Remote Sensing* 14, 1-19. https://doi.org/10.3390/rs14071727

Alves, D.B., Pérez-Cabello, F., 2017. Multiple remote sensing data sources to assess spatio-temporal patterns of fire incidence over Campos Amazônicos Savanna Vegetation Enclave (Brazilian Amazon). *Science of the Total Environment* 601-602, 142-158. https://doi.org/10.1016/j.scitotenv.2017.05.194

Alves, D.B., Alvarado, S.T., 2019. Variação espaço-temporal da ocorrência do fogo nos biomas brasileiros com base na análise de produtos de sensoriamento remoto. *Geografia* 44, 321-345. https://doi.org/10.5016/geografia.v44i2.15119

Alves, D.B., Pérez-Cabello, F., Rodrigues Mimbrero, M., 2015. Land-use and land-cover dynamics monitored by NDVI multitemporal analysis in a selected southern Amazonian area (Brazil) for the last three decades. *ISPRS - The International Archives of the Photogrammetry, Remote Sensing and Spatial Information Sciences* XL-7/W3, 329-335. https://doi.org/10.5194/isprsarchives-XL-7-W3-329-2015

Alves, D.B., Montorio Llovería, R., Pérez-Cabello, F., Vlassova, L., 2018. Fusing Landsat and MODIS data to retrieve multispectral information from fire-affected areas over tropical savannah environments in the Brazilian Amazon. *International Journal of Remote Sensing* 39, 1-23. https://doi.org/10.1080/01431161.2018.1479790

Alves, D.B., Fidelis, A., Pérez-Cabello, F., Alvarado, S.T., Conciani, D.E., Cambraia, B.C., Silveira, A.L.P. da, Silva, T.S.F., 2022. Impact of image acquisition lag-time on monitoring short-term postfire spectral dynamics in tropical savannas: the Campos Amazônicos Fire Experiment. *Journal of Applied Remote Sensing* 16, 1-24. https://doi.org/10.1117/1.jrs.16.034507

Andersen, A.N., Cook, G.D., Williams, R.J., 2003. *Fire in Tropical Savannas*: The Kapalga Experiment. Springer-Verlag, New York, USA.

Archibald, S., Lehmann, C.E.R., Belcher, C.M., Bond, W.J., Bradstock, R.A., Daniau, A.L., Dexter, K.G., Forrestel, E.J., Greve, M., He, T., Higgins, S.I., Hoffmann, W.A., Lamont, B.B., McGlinn, D.J., Moncrieff, G.R., Osborne, C.P., Pausas, J.G., Price, O., Ripley, B.S., Rogers, B.M., Schwilk, D.W., Simon, M.F., Turetsky, M.R., Van Der Werf, G.R., Zanne, A.E., 2018. Biological and geophysical feedbacks with fire in the Earth system. *Environmental Research Letters* 13. https://doi.org/10.1088/1748-9326/aa9ead

Asner, G.P., 2001. Cloud cover in Landsat observations of the Brazilian Amazon. *International Journal of Remote Sensing* 22, 3855-3862. https://doi.org/10.1080/01431160010006926

Belda, S., Pipia, L., Morcillo-Pallarés, P., Rivera-Caicedo, J.P., Amin, E., De Grave, C., Verrelst, J., 2020. DATimeS: A machine learning time series GUI toolbox for gap-filling and vegetation phenology trends detection. *Environmental Modelling & Software* 127, 104666. https://doi.org/10.1016/j.envsoft.2020.104666

Berra, E.F., Fontana, D.C., Yin, F., Breunig, F.M., 2024. Harmonized Landsat and Sentinel-2 Data with Google Earth Engine. *Remote Sensing* 16. https://doi.org/10.3390/rs16152695

Bolognesi, S.F., Pasolli, E., Belfiore, O.R., De Michele, C., D'Urso, G., 2020. Harmonized landsat 8 and sentinel-2 time series data to detect irrigated areas: An application in Southern Italy. *Remote Sensing* 12. https://doi.org/10.3390/RS12081275

Bousquet, E., Mialon, A., Rodriguez-Fernandez, N., Mermoz, S., Kerr, Y., 2022. Monitoring post-fire recovery of various vegetation biomes using multi-wavelength satellite remote sensing. *Biogeosciences* 19, 3317-3336. https://doi.org/10.5194/bg-19-3317-2022

Burton, C., Lampe, S., Kelley, D.I., Thiery, W., Hantson, S., Christidis, N., Gudmundsson, L., Forrest, M., Burke, E., Chang, J., Huang, H., Ito, A., Kou-Giesbrecht, S., Lasslop, G., Li, W., Nieradzik, L., Li, F., Chen, Y., Randerson, J., Reyer, C.P.O., Mengel, M., 2024. Global burned area increasingly explained by climate change. *Nature Climate Change* 14, 1186-1192. https://doi.org/10.1038/s41558-024-02140-w

Carneiro Filho, A., 1993. Cerrados amazônicos: fósseis vivos? Algumas reflexões. *Revista do Instituto Geológico* 14, 63-68. https://doi.org/10.5935/0100-929X.19930010

Carvalho, W.D. de, Mustin, K., 2017. The highly threatened and little known Amazonian savannahs. *Nature Ecology & Evolution* 1, 0100. https://doi.org/10.1038/s41559-017-0100

Cheney, P., Sullivan, A., 1997. *Grassfires:* Fuel, Weather and Fire Behaviour. CSIRO, Melbourne, Australia.

Chuvieco, E., Martín, M.P., Palacios, A., 2002. Assessment of different spectral indices in the red-near-infrared spectral domain for burned land discrimination. *International Journal of Remote Sensing* 23, 5103-5110. https://doi.org/10.1080/01431160210153129

Claverie, M., Ju, J., Masek, J.G., Dungan, J.L., Vermote, E.F., Roger, J.C., Skakun, S. V., Justice, C., 2018. The Harmonized Landsat and Sentinel-2 surface reflectance data set. *Remote Sensing of Environment* 219, 145-161. https://doi.org/10.1016/j.rse.2018.09.002

Claverie, M., Masek, J.G., Ju, J., Dungan, J.L., 2017. *Harmonized Landsat-8 Sentinel 2 (HLS) Product User's Guide*. https://doi.org/10.13140/RG.2.2.33017.26725

Collins, L., Trouvé, R., Baker, P.J., Cirulus, B., Nitschke, C.R., Nolan, R.H., Smith, L., Penman, T.D., 2023. Fuel reduction burning reduces wildfire severity during extreme fire events in south-eastern Australia. *Journal of Environmental Management* 343, 118171. https://doi.org/10.1016/j.jenvman.2023.118171

Coutinho, L.M., 1990. Fire in the Ecology of the Brazilian Cerrado, in: Goldammer, J.G. (Ed.), *Fire in the Tropical Biota*. Springer, Berlin, pp. 82-105. https://doi.org/10.1007/978-3-642-75395-4_6

Devries, B., Pratihast, A.K., Verbesselt, J., Kooistra, L., Herold, M., 2016. Characterizing Forest Change Using Community-Based Monitoring Data and Landsat Time Series. *PLoS One* 3, 1-25. https://doi.org/10.1371/journal.pone.0147121

ESA, European Space Agency, 2024. *Copernicus Global Digital Elevation Model*. https://doi.org/https://doi.org/10.5069/G9028PQB

Fontaine, J.B., Westcott, V.C., Enright, N.J., Lade, J.C., Miller, B.P., 2012. Fire behaviour in south-western Australian shrublands: evaluating the influence of fuel age and fire weather. *International Journal of Wildland Fire* 21, 385. https://doi.org/10.1071/WF11065

Fornacca, D., Ren, G., Xiao, W., 2018. Evaluating the Best Spectral Indices for the Detection of Burn Scars at Several Post-Fire Dates in a Mountainous Region of Northwest Yunnan, China. *Remote Sensing* 10, 1196. https://doi.org/10.3390/rs10081196

Frantz, D., 2019. FORCE-Landsat + Sentinel-2 analysis ready data and beyond. *Remote Sensing* 11. https://doi.org/10.3390/rs11091124

Fritsch, F.N., Carlson, R.E., 1980. Monotone Piecewise Cubic Interpolation. *SIAM Journal on Numerical Analysis* 17, 238-246.

Fuentes, I., Lopatin, J., Galleguillos, M., Ceballos-Comisso, A., Eyheramendy, S., Carrasco, R., 2024. Is the change deforestation? Using time-series analysis of satellite data to disentangle deforestation from other forest degradation causes. *Remote Sensing Applications: Society and Environment* 35, 101210. https://doi.org/10.1016/j.rsase.2024.101210

Funk, C., Peterson, P., Landsfeld, M., Pedreros, D., Verdin, J., Shukla, S., Husak, G., Rowland, J., Harrison, L., Hoell, A., Michaelsen, J., 2015. The climate hazards infrared precipitation with stations — a new environmental record for monitoring extremes. *Science Data* 2, 150066. https://doi.org/10.1038/sdata.2015.66

Furley, P.A., Rees, R.M., Ryan, C.M., Saiz, G., 2008. Savanna burning and the assessment of long-term fire experiments with particular reference to Zimbabwe. *Progress in Physical Geography* 32, 611-634. https://doi.org/10.1177/0309133308101383

Gitas, I., Mitri, G., Veraverbeke, S., Polychronaki, A., 2012. Advances in Remote Sensing of Post-Fire Vegetation Recovery Monitoring - A Review, in: Fatoyinbo, L. *Remote Sensing of Biomass - Principles and Applications*. InTech. https://doi.org/10.5772/20571

Gorelick, N., Hancher, M., Dixon, M., Ilyushchenko, S., Thau, D., Moore, R., 2017. Google Earth Engine: Planetary-scale geospatial analysis for everyone. *Remote Sensing of Environment* 202, 18-27. https://doi.org/10.1016/j.rse.2017.06.031

Haffer, J., Prance, G.T., 2002. Impulsos climáticos da evolução na Amazônia durante o Cenozóico: sobre a teoria dos refúgios da diferenciação biótica. *Estudos Avançados* 12. https://doi.org/10.1590/S0103-40142002000300014

Halsey, R.W., Keeley, J.E., Wilson, K., 2009. *Fuel age and fire spread: natural conditions versus opportunities for fire suppression*. U.S. Forest Service.

Hardesty, J., Myers, R., Fulks, W., 2005. Fire, ecosystems and people: a preliminary assessment of fire as a global conservation issue. *Fire Management* 22, 78-87.

Harris, S., Veraverbeke, S., Hook, S., 2011. Evaluating spectral indices for assessing fire severity in chaparral ecosystems (Southern California) using modis/aster (MASTER) airborne simulator data. *Remote Sensing* 3, 2403-2419. https://doi.org/10.3390/rs3112403

Higgins, S.I., Bond, W.J., February, E.C., Bronn, A., Euston-Brown, D.I.W., Enslin, B., Govender, N., Rademan, L., O'Regan, S., Potgieter, A.L.F., Scheiter, S., Sowry, R., Trollope, L., Trollope, W.S.W., 2007. Effects of four decades of fire manipulation on woody vegetation structure in savanna. *Ecology* 88, 1119-1125. https://doi.org/10.1890/06-1664

Hill, M.J., 2013. Vegetation index suites as indicators of vegetation state in grassland and savanna: An analysis with simulated SENTINEL 2 data for a North American transect. *Remote Sensing of Environment* 137, 94-111. https://doi.org/10.1016/j.rse.2013.06.004

Hoffmann, W.A., Adasme, R., Haridasan, M., De Carvalho, M.T., Geiger, E.L., Pereira, M.A.B., Gotsch, S.G., Franco, A.C., 2009. Tree topkill, not mortality, governs the dynamics of savanna-forest boundaries under frequent fire in central Brazil. *Ecology* 90, 1326-1337. https://doi.org/10.1890/08-0741.1

IBGE, Instituto Brasileiro de Geografia e Estatística, 2012. *Manual técnico da vegetação brasileira*. IBGE, Rio de Janeiro.

ICMBio, Instituto Chico Mendes de Conservação da Biodiversidade, 2016. *Plano de Manejo* - Parque Nacional dos Campos Amazônicos. Ministério do Meio Ambiente (MMA), Brasília, Brazil.

JT, Jupyter Team, 2015. *Jupyter Notebook Project*.

Kaufman, Y.J., Remer, L.A., 1994. Detection of forests using mid-IR reflectance: an application for aerosol studies. *IEEE Transactions on Geoscience and Remote Sensing*. 32, 672-683.

Key, C.H., Benson, N.C., 2006. Landscape assessment (LA): Sampling and analysis methods, in: Lutes, D.C., Keane, R.E., Caratti, J.F., Key, C.H., Benson, N.C., Sutherland, S., Gangi, L.J. (Eds.), *FIREMON*: Fire Effects Monitoring and Inventory System. U.S. Department of Agriculture, Forest Service, Rocky Mountain Research Station, Fort Collins, CO, USA, pp. 1-55.

Lasaponara, R., 2006. Estimating spectral separability of satellite derived parameters for burned areas mapping in the Calabria region by using SPOT-Vegetation data. *Ecological Modelling* 6, 265-270. https://doi.org/10.1016/j.ecolmodel.2006.02.025

Laurentino, J. de S., 2023. *Regeneração do estrato herbáceo após queimas experimentais no Parque Nacional dos Campos Amazônicos*. Masther's Dissertation, Universidade Estadual do Maranhão, Brasil.

Lhermitte, S., Verbesselt, J., Verstraeten, W.W., Veraverbeke, S., Coppin, P., 2011. Assessing intra-annual vegetation regrowth after fire using the pixel based regeneration index. *ISPRS Journal of Photogrammetry and Remote Sensing* 66, 17-27. https://doi.org/10.1016/j.isprsjprs.2010.08.004

MAPBIOMAS, 2023. *Projeto MapBiomas – Coleção 9.0 da série anual de mapas de cobertura e uso de solo do Brasil*. Available at: http://mapbiomas.org/ (last access: 18/03/25).

Marengo, J.A., Liebmann, B., Kousky, V.E., Filizola, N.P., Wainer, I.C., 2001. Onset and end of the rainy season in the Brazilian Amazon Basin. *Journal of Climate* 14, 833-852. https://doi.org/10.1175/1520-0442(2001)014<0833:OAEOTR>2.0.CO;2

Miranda, H.S., 2010. *Efeitos do regime do fogo sobre a estrutura de comunidades de Cerrado*: Projeto Fogo, 2ed ed. IBAMA, Brasília, Brasil.

Miranda, H.S., Silva, E.P.R., Miranda, A.C., 1996. Comportamento do fogo em queimadas de campo sujo, in: Miranda, H.S., Saito, C.H., Souza, D.B.F. (Eds.), *Impacto de Queimadas Em Áreas de Cerrado e Restinga*. Universidade de Brasília, Brasilia, Brazil, pp. 1-10.

Morton, D.C., DeFries, R.S., Nagol, J., Souza Jr., C.M., Kasischke, E.S., Hurtt, G.C., Dubayah, R., 2011. Mapping canopy damage from understory fires in Amazon forests using annual time series of Landsat and MODIS data. *Remote Sensing of Environment* 115, 1706-1720. https://doi.org/10.1016/j.rse.2011.03.002

Motta, P.E.F., Curi, N., Franzmeier, D.F., 2002. Relation of soils and geomorphic surfaces in the Brazilian Cerrado, in: Oliveira, P.S., Marquis, R.J. (Eds.), *The Cerrados of Brazil*: Ecology and Natural History of a Neotropical Savanna. Columbia University Press, New York, EUA, pp. 13-32.

Murphy, S., 2020. *Atmospheric correction of a (single) Sentinel 2 image*. Available at: https://github.com/samsammurphy/gee-atmcorr-S2 (last access: 01/03/2025)

Nguyen, M.D., Baez-Villanueva, O.M., Bui, D.D., Nguyen, P.T., Ribbe, L., 2020. Harmonization of Landsat and Sentinel 2 for crop monitoring in drought prone areas: Case studies of Ninh Thuan (Vietnam) and Bekaa (Lebanon). *Remote Sensing* 12, 1-18. https://doi.org/10.3390/rs12020281

Oliveira, U., Soares-Filho, B., Bustamante, M., Gomes, L., Ometto, J.P., Rajão, R., 2022. Determinants of Fire Impact in the Brazilian Biomes. *Frontiers in Forests and Global Change* 5, 1-12. https://doi.org/10.3389/ffgc.2022.735017

Oliveira, U., Soares-Filho, B., de Souza Costa, W.L., Gomes, L., Bustamante, M., Miranda, H., 2021. Modeling fuel loads dynamics and fire spread probability in the Brazilian Cerrado. *Forest Ecology and Management* 482, 118889. https://doi.org/10.1016/j.foreco.2020.118889

Othman, M.A., Ash'Aari, Z.H., Aris, A.Z., Ramli, M.F., 2018. Tropical deforestation monitoring using NDVI from MODIS satellite: A case study in Pahang, Malaysia. *IOP Conference Series: Earth and Environmental Science* 169. https://doi.org/10.1088/1755-1315/169/1/012047

Pacheco, A. da P., da Silva Junior, J.A., Ruiz-Armenteros, A.M., Henriques, R.F.F., de Oliveira Santos, I., 2023. Analysis of Spectral Separability for Detecting Burned Areas Using Landsat-8 OLI/TIRS Images under Different Biomes in Brazil and Portugal. *Forests* 14. https://doi.org/10.3390/f14040663

Pausas, J.G., Bond, W.J., 2020. On the Three Major Recycling Pathways in Terrestrial Ecosystems. *Trends in Ecology & Evolution* 35, 767-775. https://doi.org/10.1016/j.tree.2020.04.004

Pereira Júnior, A.C., Oliveira, S.L.J., Pereira, J.M.C., Turkman, M.A.A., 2014. Modelling fire frequency in a Cerrado savanna protected area. *PLoS One* 9. https://doi.org/10.1371/journal.pone.0102380

Pérez-Cabello, F., Montorio, R., Alves, D.B., 2021. Remote sensing techniques to assess post-fire vegetation recovery. Current Opinion in Environmental Science & Health 21, 100251. https://doi.org/10.1016/j.coesh.2021.100251

Pettorelli, N., Vik, J.O., Mysterud, A., Gaillard, J.M., Tucker, C.J., Stenseth, N.C., 2005. Using the satellite-derived NDVI to assess ecological responses to environmental change. *Trends in Ecology & Evolution* 20, 503-510. https://doi.org/10.1016/j.tree.2005.05.011

Pineda Valles, H.E., Nunes, G.M., Berlinck, C.N., Gonçalves, L.G., Ribeiro, G.H.P. de M., 2023. Use of Remotely Piloted Aircraft System Multispectral Data to Evaluate the Effects of Prescribed Burnings on Three Macrohabitats of Pantanal, Brazil. *Remote Sensing* 15, 2934. https://doi.org/10.3390/rs15112934

Pivello, V.R., 2011. The use of fire in the cerrado and amazonian rainforests of Brazil: past and present. *Fire Ecology* 7, 24-39. https://doi.org/10.4996/fireecology.0701024

Pivello, V.R., Vieira, I., Christianini, A. V., Ribeiro, D.B., da Silva Menezes, L., Berlinck, C.N., Melo, F.P.L., Marengo, J.A., Tornquist, C.G., Tomas, W.M., Overbeck, G.E., 2021. Understanding Brazil's catastrophic fires: Causes, consequences and policy needed to prevent future tragedies. *Perspectives in Ecology and Conservation* 19, 233-255. https://doi.org/10.1016/j.pecon.2021.06.005

Poortinga, A., Tenneson, K., Shapiro, A., Nquyen, Q., San Aung, K., Chishtie, F., Saah, D., 2019. Mapping Plantations in Myanmar by Fusing Landsat-8, Sentinel-2 and Sentinel-1 Data along with Systematic Error Quantification. *Remote Sensing* 11, 831. https://doi.org/10.3390/rs11070831

Prance, G.T., 1996. Islands in Amazonia. *Philosophical Transactions of the Royal Society B: Biological Sciences* 351, 823-833. https://doi.org/10.1098/rstb.1996.0077

Ratter, J.A., Bridgewater, S., Ribeiro, J.F., 2003. Analysis of the floristic composition of the Brazilian cerrado vegetation: comparison of the woody vegetation of 376 areas. *Edinburgh Journal of Botany* 57-109. https://doi.org/10.1017/S0960428603000064

RCT, R Core Team, 2019. *R*: A Language and Environment for Statistical Computing.

Rissi, M.N., Baeza, M.J., Gorgone-Barbosa, E., Zupo, T., Fidelis, A., 2017. Does season affect fire behaviour in the Cerrado? *International Journal of Wildland Fire* 26, 427-433. https://doi.org/10.1071/wf14210

Rouse, J.W., Hass, R.H., Schell, J.A., Deering, D.W., 1974. Monitoring vegetation systems in the great plains with ERTS, in: Freden, S.C., Mercanti, E.P., Becker, M.A. (Eds.), *Third Earth Resources Technology Satellite (ERTS) Symposium*. NASA Goddard Space Flight Center, Washington, DC, United States, pp. 309-317. https://doi.org/citeulike-article-id:12009708

Rowan, G.S.L., Kalacska, M., Inamdar, D., Arroyo-Mora, J.P., Soffer, R., 2021. Multi-Scale Spectral Separability of Submerged Aquatic Vegetation Species in a Freshwater Ecosystem. *Frontiers in Environmental Science* 9, 1-22. https://doi.org/10.3389/fenvs.2021.760372

Roy, D.P., Lewis, P., Schaaf, C., Devadiga, S., Boschetti, L., 2006. The Global Impact of Clouds on the Production of MODIS Bidirectional Reflectance Model-Based Composites for Terrestrial Monitoring. *IEEE Geoscience and Remote Sensing Letters* 3, 452-456. https://doi.org/10.1109/LGRS.2006.875433

Roy, D.P., Zhang, H.K., Ju, J., Gomez-Dans, J.L., Lewis, P.E., Schaaf, C.B., Sun, Q., Li, J., Huang, H., Kovalskyy, V., 2016. A general method to normalize Landsat reflectance data to nadir BRDF adjusted reflectance. *Remote Sensing of Environment* 176, 255-271. https://doi.org/10.1016/j.rse.2016.01.023

Sano, E.E., Ferreira, L.G., Asner, G.P., Steinke, E.T., 2007. Spatial and temporal probabilities of obtaining cloud-free Landsat images over the Brazilian tropical savanna. *International Journal of Remote Sensing* 28, 2739-2752. https://doi.org/10.1080/01431160600981517

Scheffler, D., Frantz, D., Segl, K., 2020. Spectral harmonization and red edge prediction of Landsat-8 to Sentinel-2 using land cover optimized multivariate regressors. *Remote Sensing of Environment* 241, 111723. https://doi.org/10.1016/j.rse.2020.111723

Scheffler, D., Hollstein, A., Diedrich, H., Segl, K., Hostert, P., 2017. AROSICS: An automated and robust open-source image co-registration software for multi-sensor satellite data. *Remote Sensing* 9. https://doi.org/10.3390/rs9070676

Schmidt, I.B., Eloy, L., 2020. Fire regime in the Brazilian Savanna: Recent changes, policy and management. *Flora* 268, 151613. https://doi.org/10.1016/j.flora.2020.151613

Senande-Rivera, M., Insua-Costa, D., Miguez-Macho, G., 2022. Spatial and temporal expansion of global wildland fire activity in response to climate change. *Nature Communications* 13, 1-9. https://doi.org/10.1038/s41467-022-28835-2

Simon, M.F., Grether, R., de Queiroz, L.P., Skema, C., Pennington, R.T., Hughes, C.E., 2009. Recent assembly of the Cerrado, a neotropical plant diversity hotspot, by in situ evolution of adaptations to fire. *Proceedings of the National Academy of Sciences* 106, 20359-20364. https://doi.org/10.1073/pnas.0903410106

Soenen, S.A., Peddle, D.R., Coburn, C.A., 2005. SCS+C: A modified sun-canopy-sensor topographic correction in forested terrain. *IEEE Transactions on Geoscience and Remote Sensing* 43, 2148-2159. https://doi.org/10.1109/TGRS.2005.852480

Torres, J., Gonçalves, J., Marcos, B., Honrado, J., 2018. Indicator-based assessment of post-fire recovery dynamics using satellite NDVI time-series. *Ecological Indicators* 89, 199-212. https://doi.org/10.1016/j.ecolind.2018.02.008

van Wilgen, B.W., Govender, N., Biggs, H.C., 2007. The contribution of fire research to fire management: a critical review of a long-term experiment in the Kruger National Park, South Africa. *International Journal of Wildland Fire* 16, 519. https://doi.org/10.1071/WF06115

Veraverbeke, S., Lhermitte, S., Verstraeten, W.W., Goossens, R., 2011. A time-integrated MODIS burn severity assessment using the multi-temporal differenced normalized burn ratio (dNBR MT). *International Journal of Applied Earth Observation and Geoinformation* 13, 52-58. https://doi.org/10.1016/j.jag.2010.06.006

Williams, P.R., Congdon, R.A., Grice, A.C., Clarke, P.J., 2003. Fire-related cues break seed dormancy of six legumes of tropical eucalypt savannas in north-eastern Australia. *Austral Ecology* 28, 507-514. https://doi.org/10.1046/j.1442-9993.2003.01307.x

Wilson, R.T., 2013. Py6S: A Python interface to the 6S radiative transfer model. Computers and Geosciences 51, 166–171. https://doi.org/10.1016/j.cageo.2012.08.002

Wulder, M.A., Hermosilla, T., White, J.C., Hobart, G., Masek, J.G., 2021. Augmenting Landsat time series with Harmonized Landsat Sentinel-2 data products: Assessment of spectral correspondence. *Science of Remote Sensing* 4, 100031. https://doi.org/10.1016/j.srs.2021.100031